Impact of Recent Research Findings on Eccentrically Braced Frame Design

PAUL RICHARDS, TAICHIRO OKAZAKI, MICHAEL ENGELHARDT, and CHIA-MING UANG

Steel eccentrically braced frames (EBF) remain a popular alternative to moment resisting and concentrically braced frames. The successful performance of EBFs under seismic loading depends on stable inelastic rotation of the links and the ability of other frame members to facilitate these link rotations. Figure 1 illustrates two typical EBF configurations with link length, *e*, and link rotation, γ, indicated.

Design provisions (AISC, 2005a) specify maximum allowable design rotations for links according to the non-dimensional link length, $e/(M_p/V_p)$. Links with $e/(M_p/V_p) < 1.6$ yield primarily in shear and are called short links. These links can be designed for 0.08-radian inelastic rotation (Figure 2). Links with $e/(M_p/V_p) > 2.6$ experience flexural yielding at the ends similar to a moment frame beam and are called long links. Long links can be designed for 0.02-radian inelastic rotation (less than the 0.03-radian inelastic rotation permitted for moment frames). Links with $e/(M_p/V_p)$ between 1.6 and 2.6 are called intermediate links and experience both flexural yielding of the flanges and shear yielding of the web. The maximum inelastic rotation for intermediate links is interpolated between 0.08 and 0.02 radian, depending on $e/(M_p/V_p)$ (Figure 2).

Paul Richards is assistant professor, department of civil and environmental engineering, Brigham Young University, Provo, UT.

Taichiro Okazaki is assistant professor, department of civil engineering, University of Minnesota, Minneapolis, MN.

Michael Engelhardt is professor, department of civil, architectural and environmental engineering, University of Texas, Austin, TX.

Chia-Ming Uang is professor, department of structural engineering, University of California, San Diego, La Jolla, CA.

Web stiffeners are required in links to delay local buckling. Kasai and Popov (1986b) developed a relationship between inelastic web buckling and stiffener spacing for links which yield in shear. This relationship, combined with an experimental study of long links by Engelhardt and Popov (1989), form the basis for stiffener spacing requirements in the 2005 AISC *Seismic Provisions for Structural Steel Buildings* (AISC, 2005a), hereafter referred to as the AISC Seismic Provisions.

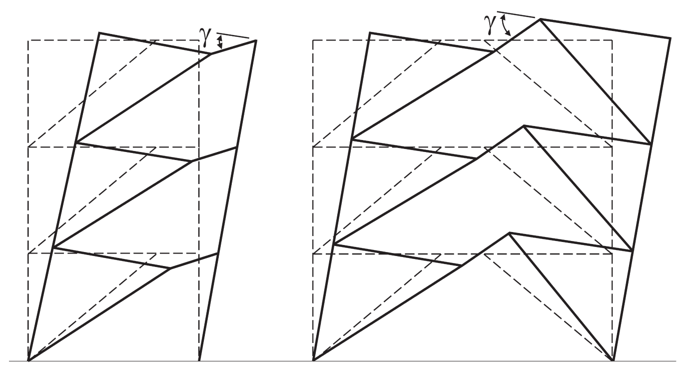

Fig. 1. Deformed geometry of typical EBFs.

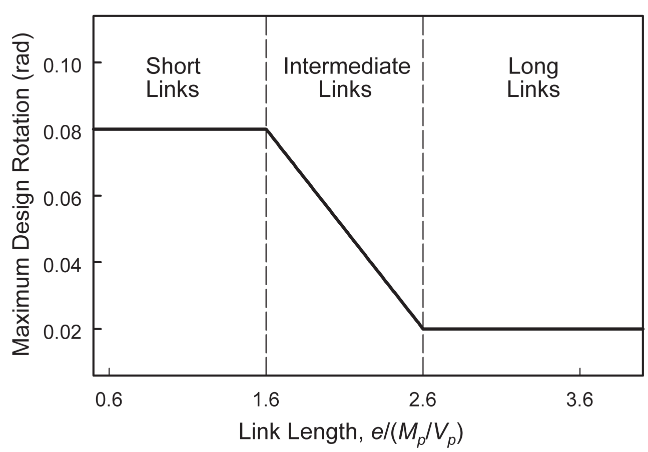

Fig. 2. Maximum design rotations (AISC, 2005a).

The previous editions of the AISC Seismic Provisions (AISC, 1997, 2002) require EBF links to comply with the same slenderness requirements as those for beams in special moment frames. Very few wide flange shapes violated the requirements when made of ASTM A36 steel. However, now that ASTM A992 has replaced A36 as the standard for steel beams, 20% of wide flange sections are disqualified for use as links by the flange width-thickness limit of $b_f/2t_f < 0.30\sqrt{E_s/F_y}$ (AISC, 1997, 2002).

Efficient EBF design becomes increasingly difficult with limited permissible link sections. Designers often find it necessary to increase link sizes to satisfy the flange width-thickness requirement (AISC, 1997, 2002), resulting in heavier columns and braces to resist the full capacity of the links. The flange width-thickness requirement for links now has significant economic impact on EBF design. It is unclear from previous studies if such a strict flange width-thickness requirement is necessary, particularly for short links, since these links yield primarily in the web and may not be affected by flange buckling.

Under earthquake loads, yielding in EBFs is intended to occur primarily within the links. To ensure that braces, columns, and the beam segments outside of the links remain essentially elastic, the maximum forces that can develop in the links must be known. The premise of current provisions is that links will have an overstrength factor of approximately 1.5 [Commentary of AISC Seismic Provisions (AISC, 2005a)].

Since 1997 there have been some experiments with links built-up from steel plates (as opposed to links made from rolled shapes such as were tested at UCB in the 1980s or UTA recently). These links were not for typical EBF frames, but were intended for bridge towers (Itani, 1997; Itani, 2002; McDaniel, Uang, and Seible, 2002) or a unique building project (Chi and Uang, 2000). These links exhibited remarkably large overstrengths, some approaching 2. These results challenge the appropriateness of the 1.5 overstrength factor, which is the basis of the AISC Seismic Provisions.

The American Institute of Steel Construction (AISC) sponsored research to investigate the impact of flange slenderness on link rotation capacity and other EBF link design issues related to the modern, higher strength steel. Experimental work was performed at the University of Texas at Austin (UTA) and analytical work was performed at the University of California, San Diego (UCSD).

EXPERIMENTAL TESTING

The UTA test set-up, illustrated in Figure 3, simulated the force and deformation environment expected in an EBF link with one of its ends attached to a column (see Figure 1, left

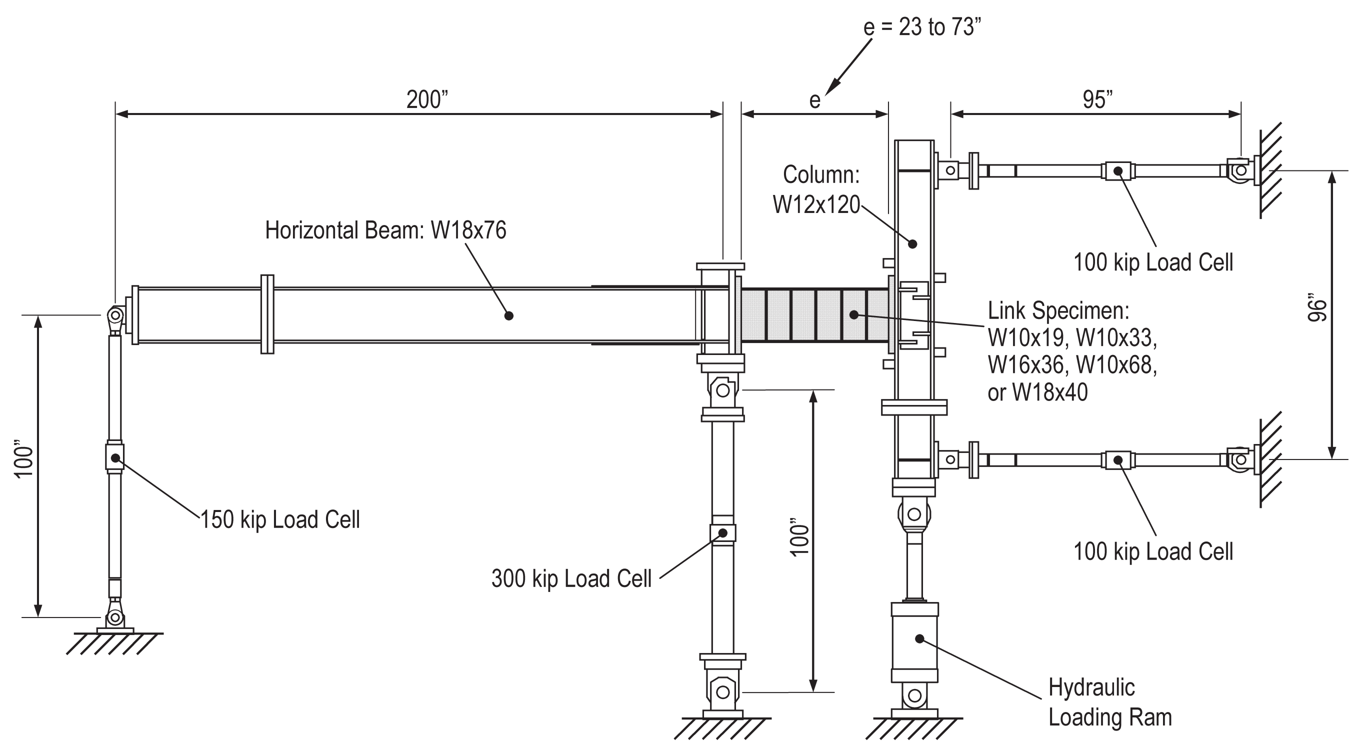

Fig. 3. University of Texas Austin (UTA) experimental set-up (Okazaki et al., 2005).

Table 1. UTA Test Specimens							
Specimen	Section	$b_f/2t_f$		Link Length, *e* (in.)	$e/(M_p/V_p)$	Intermediate Stiffeners	Loading Protocol
		Nominal	Actual				
1C	W10x19	5.09	5.22	23.0	1.73	3 @ 5¾ in.	Old AISC
2	W10x19	5.09	5.22	30.0	2.25	4 @ 6 in.	Old AISC
3	W10x19	5.09	5.22	48.0	3.61	6 in. from each end	Old AISC
4A	W10x33	9.15	9.20	23.0	1.04	3 @ 5¾ in.	Old AISC
4B	W10x33	9.15	9.20	23.0	1.04	3 @ 5¾ in.	Old AISC
4C	W10x33	9.15	9.20	23.0	1.04	3 @ 5¾ in.	Old AISC
5	W10x33	9.15	9.20	36.6	1.65	5 @ 6⅛ in.	Old AISC
6B	W10x33	9.15	9.20	48.0	2.16	4 @ 9⅝ in.	Old AISC
7	W10x33	9.15	9.20	73.0	3.29	12 in. from each end	Old AISC
8	W16x36	8.12	7.15	36.6	1.49	6 @ 5¼ in.	Old AISC
9	W16x36	8.12	7.15	48.0	1.95	5 @8 in.	Old AISC
10	W10x68	6.58	6.64	36.6	1.25	2 @12 in.	Old AISC
11	W10x68	6.58	6.64	48.0	1.64	3 @12 in.	Old AISC
12	W18x40	5.73	6.09	23.0	1.02	3 @5¾ in.	Old AISC
4A-RLP	W10x33	9.15	9.20	23.0	1.04	3 @5¾ in.	Revised
4C-RLP	W10x33	9.15	9.20	23.0	1.04	3 @5¾ in.	Revised
8-RLP	W16x36	8.12	7.15	36.6	1.49	6 @5¼ in.	Revised
9-RLP	W16x36	8.12	7.15	48.0	1.95	5 @8 in.	Revised
10-RLP	W10x68	6.58	6.64	36.6	1.25	2 @12 in.	Revised
11-RLP	W10x68	6.58	6.64	48.0	1.64	3 @12 in.	Revised
12-RLP	W18x40	5.73	6.09	23.0	1.02	3 @5¾ in.	Revised
Specimens 1A, 1B, and 6A experienced end plate failures and are not shown here.							

frame). ASTM A992 links with various lengths were fabricated using W10×19, W10×33, W10×68, W16×36 and W18×40 sections. Table 1 summarizes characteristics of the various links. The W16×36 links had measured width-thickness ratios of 7.15, just under the seismically compact limit of $0.30\sqrt{E/F_y} = 7.22$. The W10×33 links had flanges near the compact (AISC, 2005b) limit of $0.38\sqrt{E/F_y} = 9.15$. The remaining three sections had flange width-thickness ratios less than the seismically compact limit.

Details for selected specimens are shown in Figure 4. Web stiffeners were provided according to current requirements. As indicated in Figure 4(a), stiffener details were altered between selected specimens.

Two different loading protocols, shown in Figure 5, were used in the tests. The loading protocols specified the sequence of link rotation angle imposed during testing. Link rotation angle was computed as the relative displacement between the two ends of the link divided by the link length. Discussion of the two loading protocols will be provided later.

Results of the UTA tests are summarized in Table 2. The inelastic rotation evaluated from the test is shown in the second column. This inelastic rotation capacity was based on the last complete loading cycle that sustained the nominal link shear strength defined in the 2005 AISC Seismic Provisions. For comparison, the design inelastic rotation is given in the third column. Overstrength values and brief descriptions of observed failure modes are provided in the fourth and fifth columns. Test results will be discussed in the context of specific EBF issues. A more detailed description of individual test results is found in Arce (2002) and Okazaki, Arce, Ryu, and Engelhardt (2005).

FINITE ELEMENT MODELS

Finite element models of isolated links were developed using the commercial software ABAQUS (HKS, 2002). Shell elements were used for the flanges, web, and stiffeners. A typical link model is illustrated in Figure 6(b). Link rotation

Table 2. UTA Test Results				
Specimen	γ_p (rad)		Overstrength	Observed Failure Mode
	Test	Design		
1C	0.081	0.072	1.23	Flange and web buckling followed by fracture in web
2	0.070	0.041	1.24	Flange and web buckling followed by fracture in flange near link end
3	0.041	0.020	1.25	Flange and web buckling followed by fracture in flange near link end
4A	0.061	0.080	1.39	Fracture of web at stiffener weld
4B	0.071	0.080	1.42	Fracture of web at stiffener weld
4C	0.080	0.080	1.41	Fracture of web at stiffener weld
5	0.067	0.077	1.34	Fracture of web at stiffener weld
6B	0.059	0.046	1.21	Flange and web buckling followed by fracture in web
7	0.037	0.020	1.28	Flange, web, and lateral-torsional buckling
8	0.077	0.080	1.35	Flange and web buckling followed by fracture in web at stiffener weld
9	0.048	0.059	1.12	Flange and web buckling
10	0.073	0.080	1.44	Fracture of web at stiffener weld
11	0.068	0.078	1.42	Fracture of web at stiffener weld
12	0.091	0.080	1.40	Fracture of web at stiffener weld accompanied by web buckling
4A-RLP	0.120	0.080	1.45	Fracture of web at stiffener weld
4C-RLP	0.119	0.080	1.48	Fracture of web at stiffener weld
8-RLP	0.117	0.080	1.37	Flange and web buckling followed by fracture in web at stiffener weld
9-RLP	0.058	0.059	1.05	Flange and web buckling
10-RLP	0.113	0.080	1.47	Fracture of web at stiffener weld
11-RLP	0.087	0.078	1.42	Fracture of web at stiffener weld; link rotation limited by ram stroke
12-RLP	0.119	0.080	1.44	Fracture of web at stiffener weld accompanied by web buckling

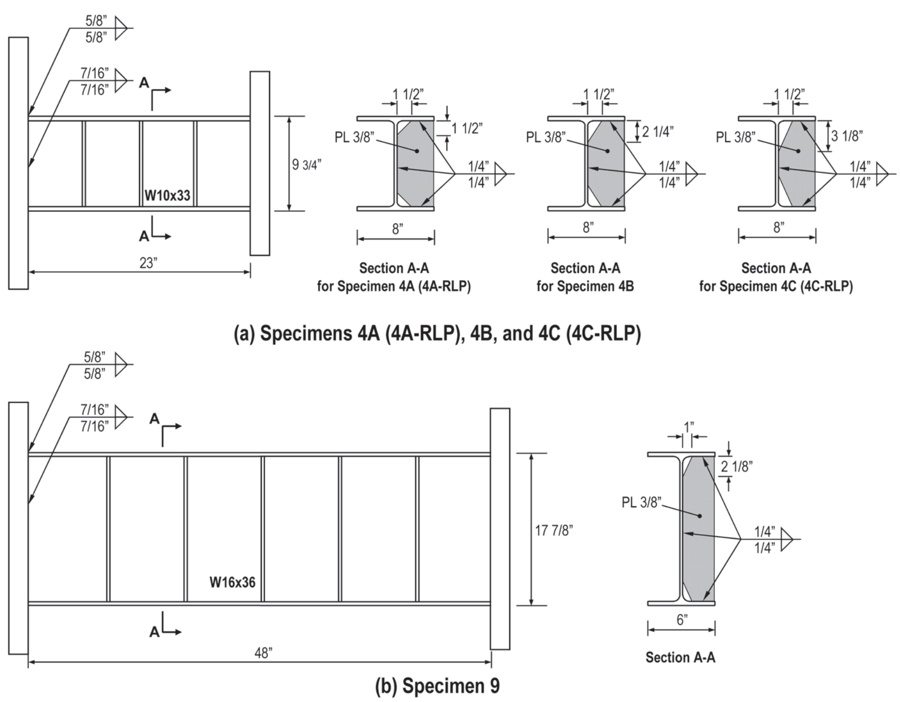

Fig. 4. Details of selected link specimens (Okazaki et al., 2005).

was applied by imposing vertical displacements on the nodes at one end of the model links, while restraining vertical displacement of the nodes at the other end. Nodes at the other end were permitted to translate horizontally but were constrained to all have the same horizontal translation. Loading in this manner resulted in constant shear along the length of the link with equal end moments and no axial forces. Links were loaded cyclically according to the protocol in the 1997 and 2002 AISC Seismic Provisions, which will be discussed here.

Plastic material response was defined using a nonlinear kinematic hardening law. Data from cyclic coupon testing performed by Kaufmann, Metrovich, and Pense (2001) were used to determine appropriate values for the parameters in the plasticity model. By including large displacement effects

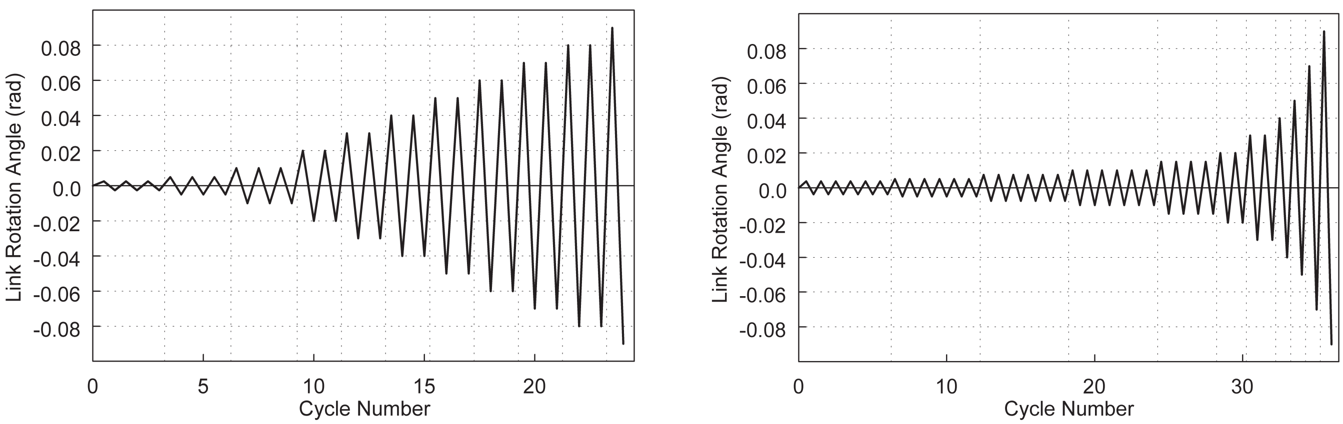

(a) Old AISC (b) Revised

Fig. 5. Experimental loading histories for links.

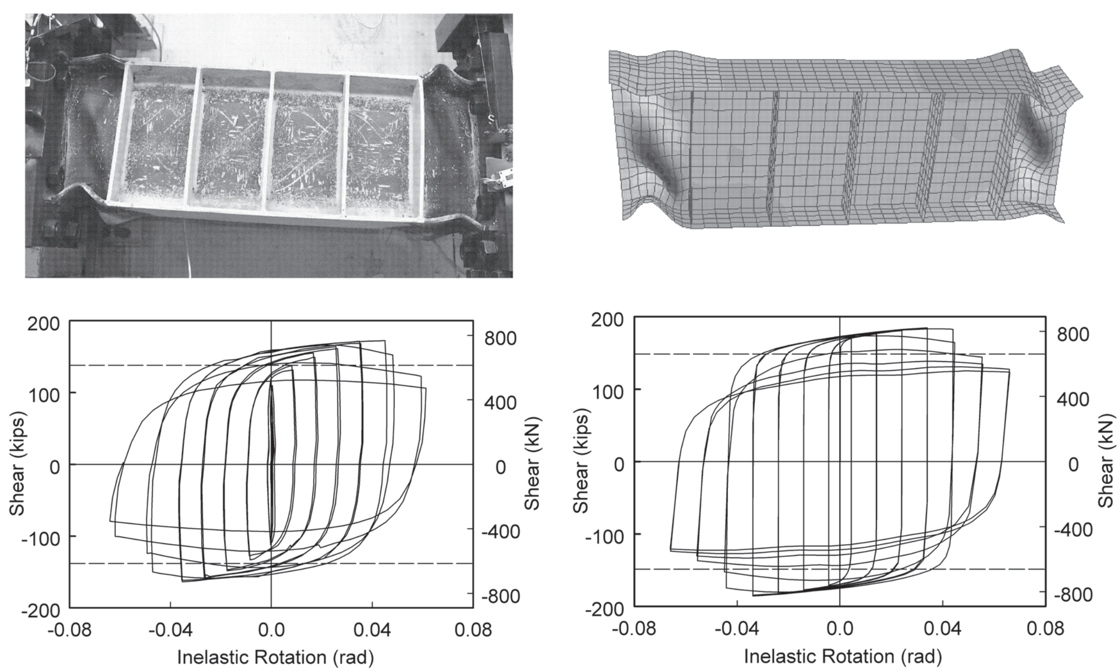

(a) Test (b) Model

Fig. 6. Deformed geometry and shear versus inelastic rotation hysteresis for UTA Specimen 9.

in the analysis, local buckling could be captured, and the post-buckling behavior of the link could be simulated.

The primary modeling objective was to accurately predict the rotation where unacceptable strength degradation resulting from severe local buckling occurs. Strength degradation associated with material failure or fracture was beyond the scope of the study. Unacceptable degradation was defined as strength loss below 80% of the maximum shear.

Models corresponding to the UTA specimens were used for a verification study. Figure 6 illustrates sample results from that study for UTA Specimen 9. The models were found to reasonably predict flange and web buckling and associated strength degradation. With verified modeling techniques, 112 unique links were analyzed under cyclic loading providing continuous data for short, intermediate, and long links with a complete range of flange width-thickness ratios. More detailed descriptions of modeling techniques and verification are found in Richards and Uang (2002).

LINK FAILURE MODES

Short links tested at UTA exhibited a failure mode not typically observed in previous link testing. The majority of the UTA short links failed due to low cycle fatigue tears in the web originating at the termination of the stiffener to web weld and propagating away from the stiffeners parallel to the flanges [Figure 7(a)]. In contrast, a typical failure mode for UCB links was web buckling followed by tearing in the buckled region [Figure 7(b)].

The failure mode observed in the UTA short links may be related to stiffener spacing. The stiffener spacing requirements found in past and present design provisions were developed at the end of the UCB link testing programs. The intent of code provisions has been to prevent web buckling in short links until they have reached 0.08-radian inelastic rotation. Since a large number of the UCB link tests in the 1980s were conducted to investigate stiffener design criteria, the majority actually did not satisfy the stiffener design guidelines that were eventually developed. The fact that few links were tested in the 1980s that satisfied the current stiffener spacing requirements may explain why this failure mode was not observed prior to the UTA tests.

An analytical investigation (Richards and Uang, 2002) found that preventing web buckling in short links results in an inelastic strain distribution in the web, where the maximum cumulative strains occur in zones running parallel to the link flanges with the greatest values at the link midspan *(Figure 8)*. In addition, material tests of the tested links indicated less ductile material near the *k*-area of the sections (Arce, 2002). The severe cyclic inelastic strain demand and the degraded material properties at the location of fracture suggest that the failure mode illustrated in Figure 7(a) is what may be reasonably expected for typical short links in EBFs. Experiments and models indicate that short links will exceed design inelastic rotations before experiencing such failures. As will be discussed later, care must be taken in interpreting the inelastic rotations listed in Table 2 since the loading protocol can substantially affect the inelastic rotation capacity obtained from experiments. Link studies, including the most recent, indicate closer stiffener spacing improves rotation capacity. While preventing web buckling changes the failure mode, it typically increases rotation capacity.

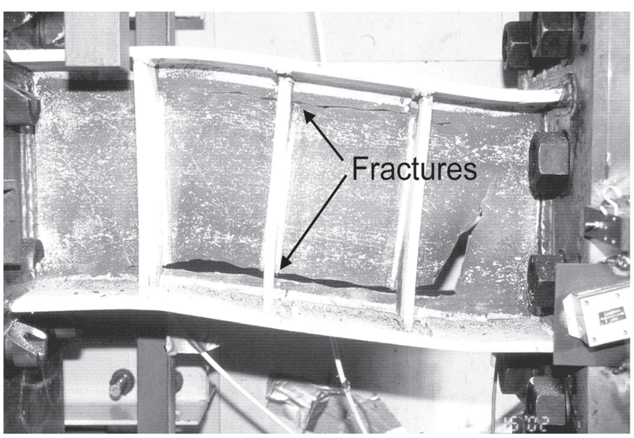

(a) Web Fractures Originating at Termination of Stiffener Welds, UTA, 4A (Arce, 2002)

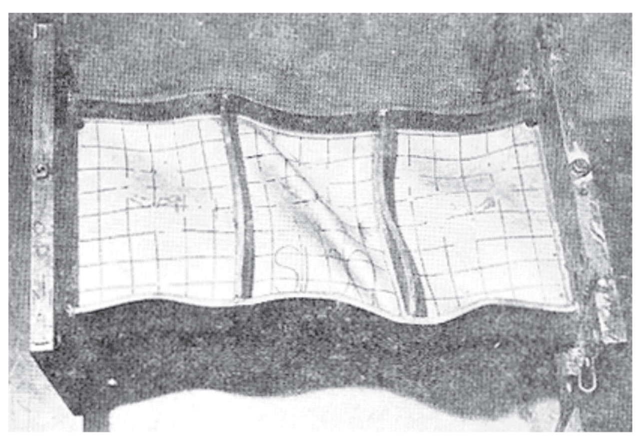

(b) Severe Buckling, UCB 20 (Malley and Popov, 1984)

Fig. 7. Short link failure modes.

The web fracture induced by low cycle fatigue, as observed in short links, was absent in intermediate and long links. Instead, these links experienced strength degradation associated with severe buckling [see Figure 6(a)] much like the long links tested by Engelhardt and Popov (1989). As illustrated in Figure 6(b), this failure mode was simulated by the finite element models with reasonable accuracy. Factors that contribute to severe buckling will be discussed shortly.

EFFECT OF EXPERIMENTAL LOADING PROTOCOL ON LINK ROTATION CAPACITY

Somewhat arbitrary and varying cyclic loading protocols were used for link testing at UCB in the 1980s. A standardized loading protocol for links first appeared in Supplement No. 2 to the 1997 AISC Seismic Provisions (AISC, 2000) [Figure 5(a)]. Initial UTA links were tested using this protocol (designated as "old AISC" in Figure 5 and Table 1). This protocol was a modified version of the SAC moment frame protocol and was not based on a study of EBF frames. The AISC protocol used in the initial UTA tests was more demanding than any of the protocols used for link testing at UCB, in that it required more inelastic cycles (Figure 9) and step increments. A large number of short links tested at UTA with this protocol did not reach the rotations observed in UCB links and did not reach rotations specified by the provisions (Table 2). The initial UTA tests brought attention to the fact that link rotation capacity is a function of the loading protocol used in testing, and a rational protocol must be used to establish link rotation capacities for design.

Since the old AISC protocol was a modified moment frame protocol and not based on EBF analysis, further work was performed at UCSD to establish a reasonable loading protocol for link testing. Time history analyses were performed for several EBF frames under a suite of design earthquakes (Richards and Uang, 2003). The loading protocol study determined that the 1997 AISC Seismic Provisions loading protocol was extremely conservative for short links,

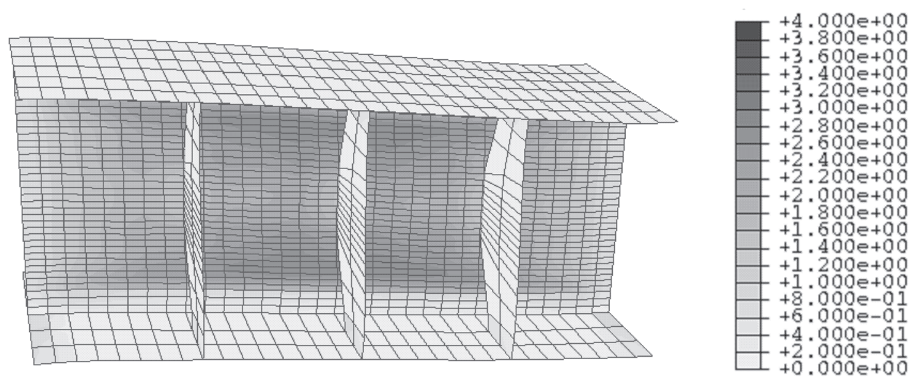

Fig. 8. Cumulative inelastic strains (PEEQ) at 0.08 radian in a link where web buckling is prevented [model of UTA 4C, Richards and Uang (2002)].

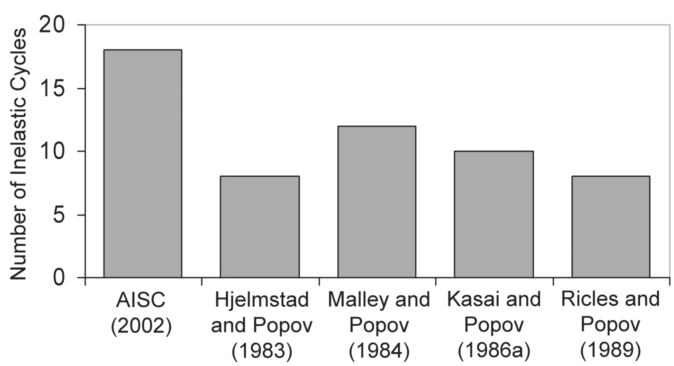

Fig. 9. Number of inelastic cycles to reach 0.08-radian inelastic rotation with various loading protocols.

somewhat conservative for intermediate links, and reasonable for long links (which are more similar to moment frame beams). A new loading protocol for testing EBF links was developed using the methodology employed by Krawinkler, Gupta, Medina, and Luco (2000) to develop the SAC loading protocol for testing beam-to-column connections in steel moment frames (AISC, 2002, 2005a). Full details of the procedure to develop the new EBF loading protocol can be found in Richards and Uang (2003). Figure 5 compares the old AISC protocol with the new, "revised" protocol for testing EBF links. Since the revised protocol is based on EBF analysis, it is believed to be more representative of demands arising from earthquake ground motion than the 1997 AISC Seismic Provisions protocol.

Five short links and two intermediate links tested with the 1997 AISC Seismic Provisions loading protocol were duplicated and retested with the new protocol (designated as Revised in Table 1) at UTA. When originally tested with the old AISC loading protocol, these specimens failed or only barely achieved the design inelastic rotation of 0.08 radian. Of the seven specimens retested with the revised protocol, all but one specimen, 9-RLP, exceeded design inelastic rotations. Figure 10 shows the shear versus inelastic rotation response of two nominally identical links tested with the different protocols. While the mode of failure was the same for both links, the link tested with the revised protocol, Specimen 4A-RLP, completed a cycle at 0.12-radian inelastic rotation, while the one tested with the old AISC protocol, Specimen 4A, failed after a cycle at 0.061 radian.

On the other hand, one intermediate link specimen, 9-RLP, did not exceed the required rotation level by an appreciable margin. Similar to its counterpart Specimen 9, the shear resistance of this specimen started to drop shortly after rising above the shear strength of the section, due to severe flange and web buckling. However, since Specimen 9-RLP retained a shear strength of 120% of its nominal shear strength at $\gamma_p = \pm 0.058$ radian, and the following strength degradation was rather gradual, the performance of this specimen was sufficient to meet the rotation requirement of $\gamma_p = \pm 0.059$ radian.

Links tested with the revised loading protocol achieved inelastic rotations that were from 19% to 97% greater than links tested with the old AISC loading protocol. The average increase in inelastic rotation using the revised loading protocol was 48%. Overall, the loading protocol study found that the protocols used in the UCB short link tests in the 1980s were reasonably conservative. The design rotation of 0.08-radian inelastic rotation for short links specified in the provisions, which is based on those results, is also reasonably conservative.

DESIGN ISSUES

Data from the UCSD models and UTA experimental links have been used to address several EBF design issues. Findings pertaining to four specific areas are discussed next: (1) impact of flange width-thickness ratio on link rotation capacity, (2) impact of stiffener spacing on intermediate link rotation capacity, (3) impact of stiffener detailing on rotation capacity, and (4) impact of link section geometry on link overstrength. Findings in each of these areas will be summarized.

Impact of Flange Width-Thickness Ratio on Rotation Capacity

The W10×33 UTA experimental specimens had flanges at the compact width-thickness limit, $b_f/2t_f$ of $0.38\sqrt{E/F_y} = 9.15$ (Table 1). Previously, EBF link sections were required to meet the seismically compact limit of $0.30\sqrt{E/F_y} = 7.22$ (AISC, 2002). The performance of the W10×33 link specimens was used to evaluate the consequences of using a link with slender flanges. The longer W10×33 specimens (Specimens 6B and 7) performed very well. These specimens exhibited

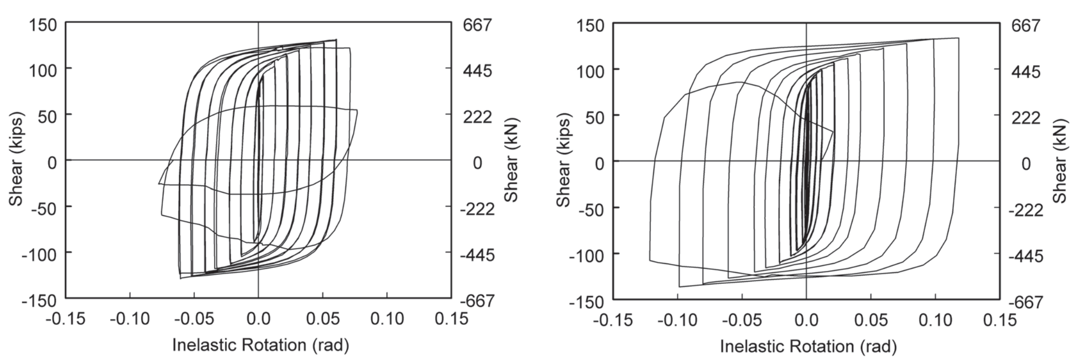

(a) UTA Specimen 4A

(b) UTA Specimen 4A-RLP

Fig. 10. Response of nominally identical links tested with different loading protocols.

flange buckling but significantly exceeded the design rotation levels before link strength dropped below the defined failure threshold (Table 2). The shorter W10×33 specimens tested using the old AISC loading protocol (Specimens 4A to 4C and 5) did not achieve their required rotations due to premature web fractures, as discussed earlier. However, when retested using the more realistic revised loading protocol, they significantly exceeded their required rotation levels. Therefore, data from the W10×33 test specimens support the adoption of the compactness limit, which is less stringent than the seismically compact limit, for the link flanges.

The W16×36 specimens had a flange width-thickness ratio right at the seismically compact limit and also provide useful data on flange slenderness effects. Of particular interest were Specimens 9 [Table 2, Figure 6(a)] and 9-RLP, which were W16×36 links with a length of $2.0M_p/V_p$. Even Specimen 9-RLP, which was tested using the revised loading protocol, only barely achieved the design inelastic rotation angle. These specimens failed due to strength degradation associated with severe combined flange and web buckling in the link end panels. Neither Specimen 9 nor 9-RLP experienced fractures in the web, so strength degradation was entirely due to local buckling. The strength degradation in the W16×36 links appeared to result from flange-web local buckling interaction. The experimental results combined with results from previous studies (Kasai and Popov, 1986a) provide strong and consistent evidence that the compactness limit is adequate for flanges of short links. The questionable performance of intermediate links with fairly slender flanges (Specimens 9 and 9-RLP) will be discussed further.

Similar to the experimental observation discussed earlier, a finite element model for Specimen 9 also experienced unacceptable strength degradation due to severe local buckling prior to reaching the design rotation [Figure 6(b)]. To investigate the extent and cause of this type of performance, a large number of finite element link models with $e/(M_p/V_p)$ between 1.6 and 2.6 with varying flange width-thickness were investigated (along with many short and long links). Figure 11 shows results from the UCSD parameter study. Short links are indicated by squares, intermediate links by triangles, and long links by circles. Solid shapes indicate models with flange width thickness ratios that satisfy current requirements. Open shapes indicate those that violate the current flange width-thickness ratio requirement.

In Figure 12 the link flange width-thickness ratio is plotted against a normalized link rotation capacity. A normalized rotation equal to or greater than one indicates the link met or exceeded the design rotation capacity indicated by the AISC Seismic Provisions (AISC, 2005a). Figure 12 does not suggest a significant relationship between flange width-thickness ratio and link rotation capacity for the links considered. A number of links (short, intermediate, and long) with extremely slender flanges achieved design rotations, while a number of intermediate links with width-thickness ratio smaller than the seismically compact limit failed to reach the design rotation. As with the experimental data, these results justify relaxation of the flange width-thickness ratio for short links and long links. Figure 12 suggests the questionable performance of some intermediate links is independent of the flange slenderness. It will be shown in the next section that the issue is related to web stiffener spacing.

Impact of Stiffener Spacing on Rotation Capacity

Figure 13(a) shows the surfaces that define the link design rotation in the AISC Seismic Provisions (AISC, 2005a).

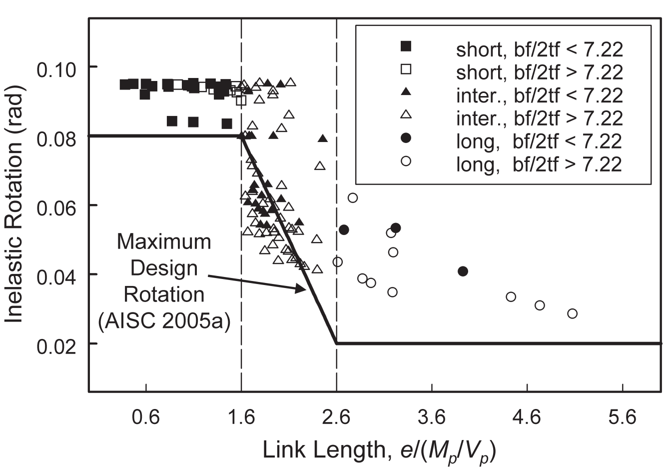

Fig. 11. Inelastic rotation capacity versus link length for finite element model links (Richards and Uang, 2005).

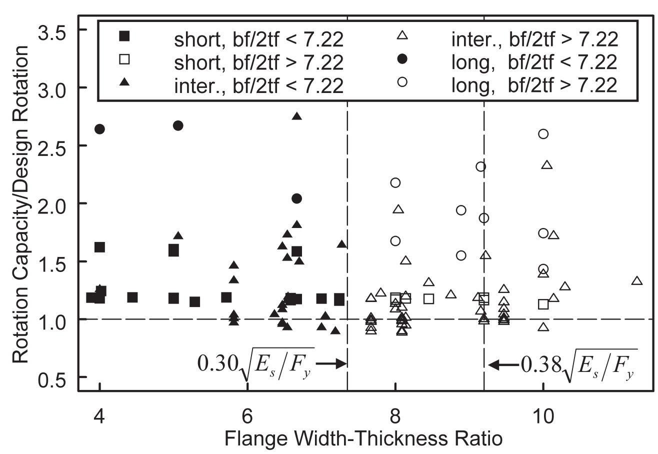

Fig. 12. Normalized inelastic rotation versus flange width-thickness ratio for model links (Richards and Uang, 2005).

Design rotation is indicated on the vertical axis. The normalized link length, $e/(M_p/V_p)$, and the normalized stiffener spacing parameter, C_B, are indicated on the horizontal axes, where

$$C_B = \left(\frac{a}{t_w}\right) + \frac{1}{5}\left(\frac{d}{t_w}\right) \tag{1}$$

where

a = stiffener spacing
t_w = web thickness
d = beam depth

Design rotations in regions A_1, A_2, and A_3 are given by the provision requirement that the design rotation shall not exceed 0.08 radian for short links, 0.02 radian for long links, and a linearly interpolated value for intermediate links. The surface in region B is implied by the requirement that intermediate stiffener spacing should not exceed $(30t_w - d/5)$ for a link rotation angle of 0.08 radian, $(52t_w - d/5)$ for link rotation angle of 0.02 radian, and a linearly interpolated value for link rotation angles between 0.08 and 0.02 radian.

Figure 13(b) shows a two-dimensional plot of the design space, with link length indicated on the horizontal axis and normalized stiffener spacing indicated on the vertical axis. Dashed lines indicate the boundaries of the surfaces shown in Figure 13(a). The data points in Figure 13(b) show the locations of the model links from this study in the design space. All of the model links that did not achieve design rotation fell in the region of the design space that is shaded in Figure 13(b). Regardless of flange width-thickness ratio, the links in this region did not achieve the design rotation while the links outside the region did.

The failure of those model intermediate links and UTA Specimens 9 and 9-RLP to reach the design rotation may be explained by the relationship between web stiffener spacing and design rotation which is assumed by the provisions [region B in Figure 13(a)]. This relationship is based on work done by Kasai and Popov for short links (Kasai and Popov, 1986b); Kasai and Popov extended elastic buckling theory for a plate in shear to the plastic case. The relationship showed very good correlation with experimental links that yielded primarily in shear. Extension of this relationship to the case of intermediate links was supported by limited available data (Engelhardt and Popov, 1989).

The web panels at both ends of intermediate links may have significant flexure-shear interaction, making them substantially more susceptible to web buckling than panels under pure shear. Figure 6 illustrates how the outside panels of an intermediate link buckle due to combined shear and flexural stresses in the web and the middle panels with the same shear stress experience no buckling. The results of this analytical study and the performance of experimental UTA Specimen 9 and 9-RLP indicate that extending the use of Kasai and Popovs' relationship to intermediate links results in somewhat unconservative design rotations for some intermediate links. It should also be noted that link models in the questionable region still achieved at least 89% of the design rotation. It is recommended, however, that conservative stiffener spacing be used for intermediate links, particularly in the end panels.

Impact of Stiffener Detailing on Rotation Capacity

The first UTA specimen to exhibit a horizontal web fracture initiating at the termination of the stiffener weld was Specimen 4A. After this failure, and based on the recommendations of McDaniel et al. (2003), the stiffener-to-link web welds were terminated at a larger distance from the flange in the subsequently tested Specimens 4B and 4C [Figure 4(a)]. In going

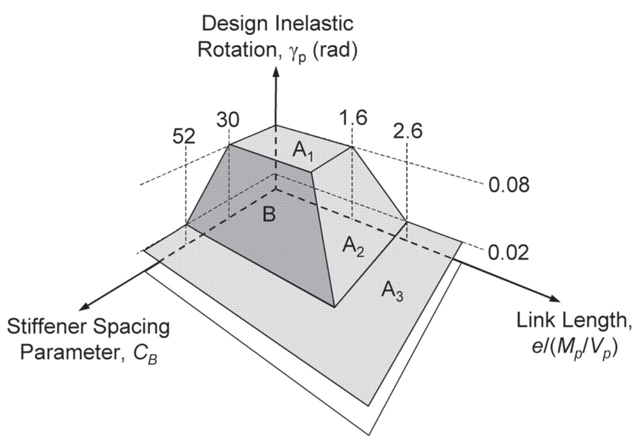

(a) Design Rotation Surfaces

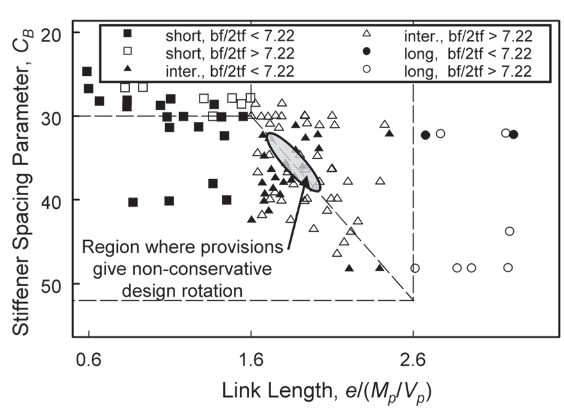

(b) Location of Model Links in Design Space

Fig. 13. Understanding intermediate link failures (Richards and Uang, 2005).

from Specimens 4A to 4B, and then to 4C, the termination of the stiffener weld was moved progressively further from the flange. In Specimen 4C, the stiffener welds were terminated a distance of approximately five times the web thickness from the *k*-line of the section (see Figure 4).

The test results (see Table 2) show that larger inelastic rotations were achieved as the stiffener welds were moved further from the *k*-line (compare 4A with 4C). However, while moving the stiffener welds further from the *k*-line was beneficial in increasing rotation capacity, it did not change the failure mode. For all specimens tested after Specimens 4A to 4C, the stiffener welds were terminated a distance of five times the web thickness from the *k*-line, but many still exhibited fractures initiating at the stiffener ends. The effect of the stiffener weld termination was not seen as clearly in the comparison between Specimens 4A-RLP and 4C-RLP. Nonetheless, based on observations from Specimens 4A, 4B, and 4C, and an analytical study by McDaniel et al. (2003), it is recommended that stiffener welds be terminated a distance of five times the web thickness from the *k*-line (Okazaki et al., 2005).

Impact of Section Geometry on Link Overstrenth

Experimental tests of links made from built-up shapes (Itani, 1997; Itani, 2002; McDaniel et al., 2003) raised concern about possible high overstrengths in links made of rolled shapes with large flange-to-web area ratios. W10×68 links were tested specifically to address this issue. This section had a ratio of flange to web area near the upper bound for rolled wide flange shapes likely to be used as links. These specimens did not show unusually large values of overstrength compared to other short link specimens. Overall, the link specimens tested at UTA exhibited similar overstrength values as previous tests (Figure 14) (Okazaki et al., 2005).

Several finite element models with very thick flanges and low $e/(M_p/V_p)$ were able to achieve large overstrengths such as those reported for the built-up links. This was due to shear carried by the link flanges after web yielding. Significant flange participation can occur only in links with $e/(M_p/V_p) < 1$ and need not be accounted for in typical EBF links (Richards, 2004). Figure 14 also indicates that the overstrength factor of 1.5 may be especially conservative for intermediate links of length near $e/(M_p/V_p) = 2$. This is likely a result of neglecting the significant shear-moment interaction in this length range in evaluating the nominal shear, V_n (Engelhardt and Popov, 1989).

SUMMARY AND CONCLUSIONS

Recent experimental work performed at the University of Texas at Austin and analytical work performed at the University of California, San Diego address EBF design issues.

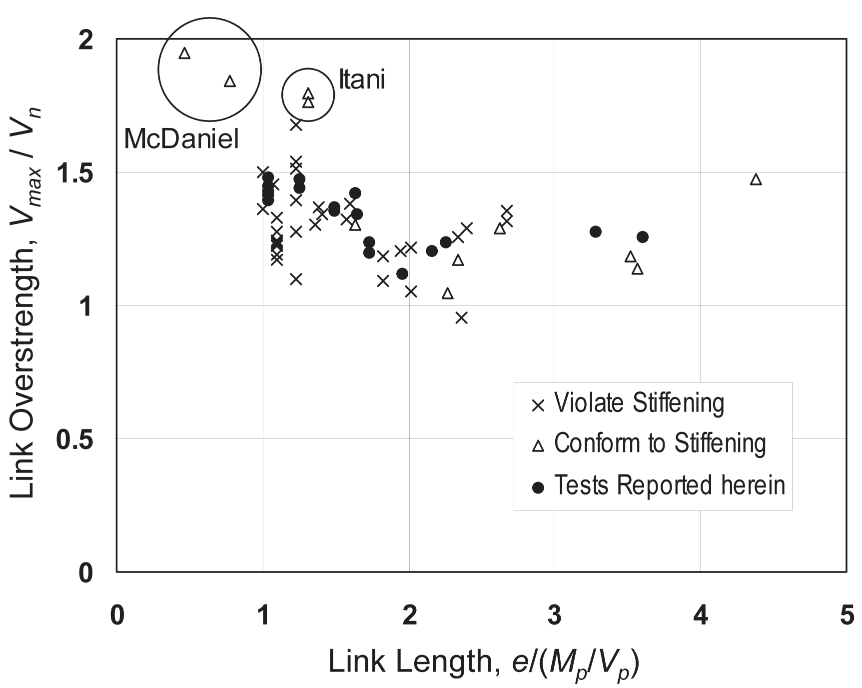

Fig. 14. Link overstrength (Okazaki et al., 2005).

From these studies, the following conclusions can be made:

- Failure of short links constructed of A992 steel and designed according to current provisions is likely dominated by web fractures that initiate at the stiffener weld termination points. Short link failures due to severe web buckling, as observed in past tests, was not observed in recent tests. Despite the change in failure mode, the short links were found to satisfy the inelastic rotation requirements.

- Link rotation capacity can be improved by terminating welds connecting intermediate stiffeners to the link web at a distance of five times the web thickness away from the *k*-line of the link section. Commentary in the 2005 AISC Seismic Provisions recommends avoiding welding in the *k*-area.

- The experimental and analytical studies reported herein as well as results from previous tests consistently support that the flange width-thickness limit of $0.38\sqrt{E/F_y}$ (compactness limit) is adequate to control flange buckling in short links. However, it is not clear whether the relaxed flange width-thickness limit is justified for intermediate and long links. The 2005 AISC Seismic Provisions permit the use of the compactness limit for short links.

- Intermediate links are susceptible to strength degradation associated with combined flange and web buckling.

- Link rotation capacity is dependent on the loading protocol used for testing. The EBF protocol in the 1997 and 2002 AISC Seismic Provisions was overly conservative. The revised protocol developed in this program is more reasonable to represent demands arising from actual earthquake ground motions. The link loading protocol in the 2005 AISC Seismic Provisions is based on the revised protocol.

- ASTM A992 links have similar overstrength to A36 links tested in the past. The flanges of links with $e/(M_p/V_p) < 1$ may carry shear forces that should be accounted for in computing ultimate shear strength.

Further details of the studies reported herein are provided in the references and other forthcoming publications.

ACKNOWLEDGMENTS

Primary funding for this research was provided by the American Institute of Steel Construction with Mr. Tom Schlafly as the project manager. Supplemental funding for the experimental work at the University of Texas, Austin came from the National Science Foundation (Grant No. CMS-0000031). Dr. Subhash Goel, Mr. James Malley, and Dr. Tom Sabol provided guidance and professional perspective on the project. Dr. Helmut Krawinkler provided guidance on the development of link test loading protocol.

REFERENCES

AISC (1997), *Seismic Provisions for Structural Steel Buildings,* American Institute of Steel Construction, Inc., Chicago, IL.

AISC (2000), *Seismic Provisions for Structural Steel Buildings (1997) Supplement No. 2*, American Institute of Steel Construction, Inc., Chicago, IL.

AISC (2002), *Seismic Provisions for Structural Steel Buildings,* ANSI/AISC 341-02, American Institute of Steel Construction, Inc., Chicago, IL.

AISC (2005a), *Seismic Provisions for Structural Steel Buildings,* ANSI/AISC 341-05, American Institute of Steel Construction, Inc., Chicago, IL.

AISC (2005b), *Specification for Structural Steel Buildings,* ANSI/AISC 360-05, American Institute of Steel Construction, Inc., Chicago, IL.

Arce, G. (2002), "Impact of Higher Strength Steels on Local Buckling and Overstrength of Links in Eccentrically Braced Frames," Masters Thesis, University of Texas at Austin, Austin, TX (advisor: M.D. Engelhardt).

Chi, B. and Uang, C.-M. (2000), "Cyclic Testing of Steel Shear Links for the San Francisco Moscone Convention Center Expansion Project," *Report No. TR-99/06,* Department of Structural Engineering, University of California, San Diego, La Jolla, CA.

Engelhardt, M.D. and Popov, E.P. (1989), "Behavior of Long Links in Eccentrically Braced Frames," *Report No. UCB/EERC-89/01,* Earthquake Engineering Research Center, University of California at Berkeley, Richmond, CA.

Hjelmstad, K.D. and Popov, E.P. (1983), "Cyclic Behavior and Design of Link Beams," *Journal of Structural Engineering,* ASCE, Vol. 109, No. 10, pp. 2387–2403.

HKS (2002), *ABAQUS Standard Users Manual, Volumes I and II,* Version 6.2, Hibbitt, Karlsson and Sorensen, Inc., Providence, RI.

Itani, A.M. (1997), "Cyclic Behavior of Richmond-San Rafael tower Links," *Report No. CEER 97-4,* Center for Civil Engineering Earthquake Research, University of Nevada at Reno, Reno, NV.

Itani, A.M. (2002), "Cyclic Behavior of Shear Links and Tower Shaft Assembly of San Francisco-Oakland Bay Bridge Tower," *Report No. CCEER 02-06,* Center for Civil Engineering Earthquake Research, Department of Civil Engineering, University of Nevada at Reno, Reno, NV.

Kasai, K. and Popov, E.P. (1986a), "General Behavior of WF Steel Shear Link Beams," *Journal of Structural Engineering,* ASCE, Vol. 112, No. 2, pp. 362–363.

Kasai, K. and Popov, E.P. (1986b), "Cyclic Web Buckling Control for Shear Link Beams," *Journal of Structural Engineering,* ASCE, Vol. 112, No. 3, pp. 505–523.

Kaufmann, E.J., Metrovich, B.R., and Pense, A.W. (2001), "Characterization of Cyclic Inelastic Strain Behavior on Properties of A572 Gr. 50 and A913 Gr. 50 Rolled Sections," *ATLSS Report No. 01-13,* National Center for Engineering Research on Advanced Technology for Large Structural Systems, Lehigh University, Bethlehem, PA.

Krawinkler, H., Gupta, A., Medina, R., and Luco, N. (2000), "Loading Histories for Seismic Performance Testing of SMRF Components and Assemblies," *Report No. SAC/BD-00/10,* SAC Joint Venture.

Malley, J.O. and Popov, E.P. (1984), "Shear Links in Eccentrically Braced Frames," *Journal of Structural Engineering,* ASCE, Vol. 110, No. 9, pp. 2275–2295.

McDaniel, C.C., Uang, C.-M., and Seible, F. (2003), "Cyclic Testing of Built-Up Steel Shear Links for the New Bay Bridge," *Journal of Structural Engineering,* ASCE, Vol. 129, No. 6, pp. 801–809.

Okazaki, T., Arce, G., Ryu, H.-C., and Engelhardt, M.D. (2005), "Experimental Study of Local Buckling, Overstrength, and Fracture of Links in Eccentrically Braced Frames," *Journal of Structural Engineering,* ASCE, Vol. 131, No. 10, pp. 1526–1535.

Richards, P. and Uang, C.-M. (2002), "Evaluation of Rotation Capacity and Overstrength of Links in Eccentrically Braced Frames (Phase 1)," *Report No. SSRP-2002/18,* Department of Structural Engineering, University of California at San Diego, La Jolla, CA.

Richards, P. and Uang, C.-M. (2003), "Development of Testing Protocol for Short Links in Eccentrically Braced Frames," *Report No. SSRP-2003/08,* Department of Structural Engineering, University of California at San Diego, La Jolla, CA.

Richards, P. (2004), "Cyclic Stability and Capacity Design of Steel Eccentrically Braced Frames," Dissertation, University of California, San Diego, CA (advisor: C.-M. Uang).

Richards, P. and Uang, C.-M. (2005), "Effect of Flange Width-Thickness Ratio on Eccentrically Braced Frames Link Cyclic Rotation Capacity," *Journal of Structural Engineering,* ASCE, Vol. 131, No. 1, pp. 1546–1547.

Ricles, J.M. and Popov, E.P. (1989), "Composite Action in Eccentrically Braced Frames," *Journal of Structural Engineering,* ASCE, Vol. 115, No. 8, pp. 2046–2066.